

Simultaneous Transmitting and Reflecting Intelligent Surfaces-Empowered NOMA Networks

Mahmoud Aldababsa, Aymen Khaleel, *Student Member, IEEE* and Ertugrul Basar, *Senior Member, IEEE*

Abstract—In this paper, we propose simultaneous transmitting and reflecting reconfigurable intelligent surface (STAR-RIS) assisted non-orthogonal multiple access (NOMA) networks. The considered STAR-RIS utilizes the mode switching (MS) protocol to serve multiple NOMA users located on both sides of the RIS surface. Based on the MS protocol, each STAR-RIS element can operate in full transmission or reflection mode. Within this perspective, we propose a novel algorithm to partition the STAR-RIS surface among the available users. This algorithm aims to determine the proper number of transmitting/reflecting elements needs to be assigned to each user in order to maximize the system sum-rate while guaranteeing the quality-of-service requirements for individual users. For the proposed system, we derive closed-form analytical expressions for the outage probability (OP) and its corresponding asymptotic behavior under different user deployments. Finally, Monte Carlo simulations are performed in order to verify the correctness of the theoretical analysis. It is shown that the proposed system outperforms the classical NOMA and orthogonal multiple access systems in terms of OP and sum-rate.

Index Terms—Simultaneous transmitting and reflecting reconfigurable intelligent surface (STAR-RIS), non-orthogonal multiple access (NOMA), mode switching (MS) protocol, outage probability (OP).

I. INTRODUCTION

Reconfigurable intelligent surface (RIS)-empowered communication has been considered as a promising candidate to enhance the performance of future wireless networks in terms of energy efficiency and coverage [1]-[2]. Basically, an RIS consists of massive low-cost reconfigurable passive elements by which it can reconfigure the propagation of incident wireless signals by adjusting the amplitude and phase shift of each individual element [3]. RISs do not require radio frequency (RF) chains, rather, they process the impinging signal over-the-air. This remarkably reduces the energy consumption and hardware costs, and hence, makes RISs economical and environmentally friendly compared to multi-antenna and relaying systems [4]. Despite the aforementioned advantages, RISs act as reflective metasurfaces, which means that RISs can only serve the users located on their same side. In other words, RISs offer only half-space coverage, which limits the flexibility of deploying them. To solve this problem, recently, the novel concept of simultaneous transmitting and reflecting RISs (STAR-RISs) has been proposed [5]. Compared to conventional RISs, STAR-RISs have elements that support both electric polarization and magnetization currents yielding simultaneous control of the transmitted and reflected signals. In this way, STAR-RISs can offer full-space coverage. Furthermore, in order to enhance this full-space coverage, three main operating protocols are proposed, namely the energy splitting (ES), mode

switching (MS), and time switching (TS). Specifically, for ES, all elements of the STAR-RIS are assumed to operate in transmission and reflection mode simultaneously. For MS, each element can operate in full transmission or reflection mode, while in TS, all elements periodically switch between the transmission and reflection modes in an orthogonal time slots.

Non-orthogonal multiple access (NOMA) has also received significant attention due to its ability to realize high spectral efficiency, massive connectivity, and low latency [6]. NOMA is fundamentally different than conventional orthogonal multiple access (OMA) schemes which provide orthogonal access to the users either in time, frequency, code, or space. The key idea in NOMA is to allocate non-orthogonal resources to serve multiple users, yielding a higher spectral efficiency while allowing some degree of interference at receivers [7]. In power-domain NOMA (PD-NOMA), multiple users' signals are superposed with different power levels that are in reverse order to their channels' gains. At the receiver side, successive interference cancellation (SIC) is applied by each user to recover its own signal, providing a good trade-off between system throughput and user fairness [8].

A. Related Works

Since the concept of STAR-RIS is relatively new, only a few works in the literature have investigated it so far [9]-[12]. Particularly, in [9], a general hardware model for STAR-RISs was introduced. The channel models for the near- and far-field regions of STAR-RISs were also investigated and the analytical expressions for the channel gains of users were derived in closed-form. Next, the active and passive beamforming optimization problem was considered in [10] for the STAR-RIS-assisted downlink networks in both unicast and multicast transmission cases. Especially, for three practical operating protocols ES, MS, and TS, the active beamforming at the BS and the passive transmission/reflection beamforming at the STAR-RIS were jointly optimized in order to minimize the power consumption of the BS and satisfy the quality-of-service (QoS) requirements of the users. Then, the weighted sum-rate maximization problem of the STAR-RIS-assisted MIMO networks was studied in [11]. Here, the authors proposed an alternative block coordinate descent algorithm to design the precoding matrices and the transmitting/reflecting coefficients. In [12], practical hardware implementations and their accurate physical models were investigated for STAR-intelligent omni surfaces (STAR-IOSs).

Due to their remarkable advantages, the integration of RISs with NOMA systems is indispensable in future wireless

communications to fulfill the stringent demands on data rate and connectivity [6]. Motivated by this, recent research efforts have been devoted to STAR-RIS assisted NOMA systems [13]-[18]. Particularly, the authors in [13] maximized the coverage range of STAR-RIS aided two-user communication networks for both NOMA and OMA by jointly optimizing the resource allocation at the BS and the transmission/reflection coefficients at the STAR-RISs. Next, the authors in [14] exploited a STAR-RIS in NOMA enhanced coordinated multi-point transmission networks in order to eliminate and boost the inter-cell interferences and desired signals, respectively. Then, in [15], by jointly optimizing the decoding order, power allocation coefficients, active beamforming, and transmission/reflection beamforming, the achievable sum-rate was maximized for the STAR-RIS-assisted NOMA system. The authors in [16] used a STAR-RIS to enable a heterogeneous network that integrated uplink NOMA and over-the-air federated learning into a unified framework to address the scarcity of system bandwidth. In addition, they minimized the optimality gap while guaranteeing QoS requirements by jointly optimizing the transmit power at users and the configuration mode at the STAR-RIS. Finally, for the sake of deriving approximated mathematical channel models for STAR-RISs, the authors exploited the central limit, curve fitting and M-fold convolution models in [17] while central limit theorem (CLT) and channel power gain models are used in [18].

B. Motivation and Contributions

It is worth mentioning that the aforementioned STAR-RIS assisted NOMA works mainly focus on the coverage range maximization [13], interference mitigation [14], sum-rate maximization [15], optimality gap minimization [16] and obtaining tractable channel models [17]-[18]. However, STAR-RIS partitioning problem and STAR-RIS element-wise mode selection have not been addressed yet.

To the best of our knowledge and with the above motivation, for the first time in the literature, we propose a STAR-RIS partitioning algorithm for a downlink STAR-RIS assisted NOMA network. In this network, the BS communicates multiple users with the assistance of a STAR-RIS. The users are assumed to be randomly deployed on the transmission and reflection sides of the STAR-RIS. According to the STAR-RIS MS protocol, each element of the STAR-RIS can operate in transmission or reflection mode. Therefore, in order to serve the users on both sides of the STAR-RIS, we propose a novel algorithm to partition the RIS surface among users on two stages. First, the RIS surface is partitioned into two parts, transmission and reflection parts, which contain all the elements that operate in transmission and reflection modes, respectively. Second, each STAR-RIS part is partitioned into subsurfaces, where each subsurface is allocated to serve a specific user located on the side of that part. Consequently, the proposed partitioning algorithm aims to determine the proper number of transmitting/reflecting STAR-RIS elements needs to be assigned to each user in order to maximize sum-rate while guaranteeing QoS requirements for the users. The main contributions of the paper can be summarized as follows:

- We introduce a novel STAR-RIS assisted NOMA system where each user is assigned to a different partition (subsurface) of the STAR-RIS and thus, the passive beamforming is performed for each user independently from the other users.
- We propose a novel algorithm to partition the STAR-RIS surface among users on two stages, in order to maximize the system sum-rate while fulfilling the different QoS requirements for different users.
- We derive exact and asymptotic expressions of the OP for the STAR-RIS aided NOMA network under different user deployments.
- We verify the theoretical results by Monte Carlo simulations. Furthermore, with comprehensive computer simulations, we show the superiority of the proposed STAR-RIS assisted NOMA network over the classical NOMA and OMA systems in terms of OP and sum-rate.

C. Paper Organization and Notations

The organization of the paper is given as follows: In Section II, the system model of the STAR-RIS assisted NOMA network is described. The OP analysis is conducted in Section III. In Section IV, the STAR-RIS partitioning algorithm is presented. In Section V, the numerical results are demonstrated and in Section VI, the paper is concluded.

Notations: Matrices and vectors are denoted by an upper and lower case boldface letters, respectively. $\mathbf{X} \in \mathbb{C}^{m \times n}$ denotes a matrix \mathbf{X} with $m \times n$ size. $[\mathbf{x}]_n$ denotes the n th entry of a vector \mathbf{x} . $|\cdot|$, $E[\cdot]$, $\lceil \cdot \rceil$ and $(\cdot)^H$ represent the absolute value, expectation operator, ceiling operator and Hermitian transpose, respectively. $P_r(\cdot)$ symbolizes probability. $F_X(x)$ denotes cumulative distribution function (CDF) of a random variable X . $\mathcal{CN}(\mu, \sigma^2)$ stands for the complex Gaussian distribution with mean μ and variance σ^2 . $Q_m(\cdot, \cdot)$ refers to the m th order generalized Marcum Q-function.

II. STAR-RIS NOMA NETWORK: SYSTEM MODEL

Consider a downlink STAR-RIS assisted multi-user wireless network where a single-antenna base station (BS) and an RIS with N elements serve K single-antenna users by using PD-NOMA, as shown in Fig. 1. The users are grouped into two main clusters, C_t and C_r , which contain K_t users located in the transmission region and K_r users located in the reflection region of the RIS, respectively. In order to serve the users in both clusters, the RIS is partitioned into two main parts, where the first and second parts contain N_t and N_r elements to serve the users in C_t and C_r , respectively. The elements in the first and second parts are operated in the transmission (t) and reflection (r) modes, respectively, and the whole RIS is assumed to be deployed in the far-field of the BS. Furthermore, the transmission and reflection parts of the RIS are partitioned into subsurfaces, where each subsurface is allocated to serve a specific user in the transmission or reflection region. The BS- U_k direct link is assumed to be blocked by obstacles, where U_k stands for the user k , $k \in \mathbb{K}_\chi$, note that $\chi \in \{t, r\}$, $\mathbb{K}_t = \{1, \dots, K_t\}$ and $\mathbb{K}_r = \{K_t + 1, \dots, K_t + K_r\}$. The BS-RIS link is assumed to have a Rayleigh fading channel model,

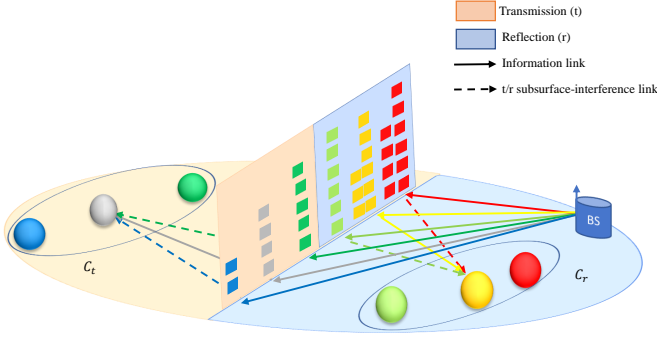


Fig. 1: An STAR-RIS aided multi-user downlink communication system model.

where $\mathbf{h}^i \in \mathbb{C}^{N_\chi^i \times 1}$ denotes the BS- i th subsurface channel vector, N_χ^i refers to the number of elements that belong to the i th subsurface in the transmission or reflection part of the RIS, and $[\mathbf{h}^i]_n = h^{i,n}$. Here, $h^{i,n} = \sqrt{L_{BS}} \zeta_\chi^{i,n} e^{-j\phi_\chi^{i,n}}$, where L_{BS} , $\zeta_\chi^{i,n}$, and $\phi_\chi^{i,n}$ denote the path gain, channel amplitude, and channel phase, respectively, and $h^{i,n} \sim \mathcal{CN}(0, L_{BS})$. Likewise, the RIS- U_k link is assumed to have Rayleigh fading channel model, where the channel vector between the i th subsurface in the transmission or reflection part of the RIS and U_k is denoted by $\mathbf{g}_{\chi,k}^i$, where $[\mathbf{g}_{\chi,k}^i]_n = g_{\chi,k}^{i,n}$ and $\chi \in \{t, r\}$. Here, $g_{\chi,k}^{i,n} = \sqrt{L_{SU,\chi,k}} \eta_{\chi,k}^{i,n} e^{-j\varphi_{\chi,k}^{i,n}}$, where $L_{SU,\chi,k}$, $\eta_{\chi,k}^{i,n}$, and $\varphi_{\chi,k}^{i,n}$ denote the path gain, channel amplitude, and channel phase, respectively, and $g_{\chi,k}^{i,n} \sim \mathcal{CN}(0, L_{SU,\chi,k})$. The transmission/reflection coefficients for the i th subsurface in the transmission or reflection part of the RIS are denoted by the entries of the diagonal matrix $\Theta_\chi^i \in \mathbb{C}^{N_\chi^i \times N_\chi^i}$, for the n th element we have $[\Theta_\chi^i]_n = \beta_\chi^{i,n} e^{j\theta_\chi^{i,n}}$, where $\theta_\chi^{i,n} \in [0, 2\pi)$ and $\beta_\chi^{i,n} = 1$, under the full transmission/reflection assumption.

Considering PD-NOMA, the BS transmits the signal x , which superimposes the K_t and K_r users' symbols, as follows:

$$\begin{aligned} x &= \sum_{k=1}^K \sqrt{a_k P} x_k \\ &= \sum_{k=1}^{K_t} \sqrt{a_k P} x_k + \sum_{k=K_t+1}^{K_t+K_r} \sqrt{a_k P} x_k, \end{aligned} \quad (1)$$

where P is the BS transmit power, x_k and a_k are the user k 's symbol and power allocation factor, respectively, $\mathbb{E}[|x_k|^2] = 1$, $\sum_{k=1}^K a_k = 1$. The users are ordered according to their channel gains as $\{U_1, \dots, U_{K_t}, U_{K_t+1}, \dots, U_{K_t+K_r}\}$, where U_1 and $U_{K_t+K_r}$ are the users with the weakest and strongest channel gains, respectively. Thus, the power allocation coefficients are ordered as $a_1 \geq \dots \geq a_k \geq \dots \geq a_K$. By using the SIC process, each user first decodes all strongest signals' users and subtracts them from the received signal, and finally, it decodes its own message. Specifically, the k th user cancels the interfered signals from U_1, \dots, U_{k-1} and treats U_{k+1}, \dots, U_K as interference. Accordingly, considering successful SIC process

at the k th user, the received signal can be expressed as

$$\begin{aligned} y_k &= \underbrace{(\mathbf{g}_{\chi,k}^k)^T \Theta_\chi^k \mathbf{h}_\chi^k \sqrt{a_k P} x_k}_{\text{Desired signal term}} + \underbrace{(\mathbf{g}_{\chi,k}^k)^T \Theta_\chi^k \mathbf{h}_\chi^k \sum_{l=k+1}^K \sqrt{a_l P} x_l}_{\text{User-interference term}} \\ &+ \underbrace{\sum_{\substack{i \in \mathbb{K}_\chi \\ i \neq k}} (\mathbf{g}_{\chi,k}^i)^T \Theta_\chi^i \mathbf{h}_\chi^i x_i}_{\text{Subsurface-interference term}} + n_k, \end{aligned} \quad (2)$$

where the first three terms in (2) denote the desired signal of the k th user, the interference of other users, and the subsurfaces mutual interference within the transmission or reflection part of the RIS, respectively, while n_k denotes the complex additive white Gaussian noise (AWGN) sample with zero mean and variance σ_k^2 at the k th user, $n_k \sim \mathcal{CN}(0, \sigma_k^2)$.

By letting $r_{\chi,k}^k = (\mathbf{g}_{\chi,k}^k)^T \Theta_\chi^k \mathbf{h}_\chi^k$, $r_{\chi,k}^i = (\mathbf{g}_{\chi,k}^i)^T \Theta_\chi^i \mathbf{h}_\chi^i$, $\sigma_k^2 = \sigma^2$, and defining $\rho = \frac{P}{\sigma^2}$ is the transmit SNR, then the signal-to-interference-plus-noise ratio (SINR) for user k to detect user j 's signal γ_j^k , $\{j \leq k, j \neq K\}$, can be obtained from (2) as

$$\gamma_j^k = \frac{\rho |r_{\chi,k}^k|^2 a_j}{\rho |r_{\chi,k}^k|^2 \sum_{l=j+1}^K a_l + \rho \left| \sum_{\substack{i \in \mathbb{K}_\chi \\ i \neq k}} r_{\chi,k}^i \right|^2 + 1}. \quad (3)$$

In order to assure that each subsurface i serves user $k = i$, its phase shifts are adjusted to remove the overall BS-STAR-RIS- U_k channel phases and maximize γ_j^k as follows:

$$\theta_\chi^{k,n} = \phi_\chi^{k,n} + \varphi_{\chi,k}^{k,n}, \quad (4)$$

by considering (4), $|r_{\chi,k}^k|^2$ and $\left| \sum_{\substack{i \in \mathbb{K}_\chi \\ i \neq k}} r_{\chi,k}^i \right|^2$ can be re-expressed, respectively, as

$$|r_{\chi,k}^k|^2 = \left| \sqrt{L_k} \sum_{n=1}^{N_\chi^k} \zeta_\chi^{k,n} \eta_{\chi,k}^{k,n} \right|^2, \quad (5)$$

$$\left| \sum_{\substack{i \in \mathbb{K}_\chi \\ i \neq k}} r_{\chi,k}^i \right|^2 = \left| \sqrt{L_k} \sum_{\substack{i \in \mathbb{K}_\chi \\ i \neq k}} \sum_{n=1}^{N_\chi^i} \zeta_\chi^{i,n} \eta_{\chi,k}^{i,n} e^{j\Phi_{\chi,k}^{i,n}} \right|^2, \quad (6)$$

where $\Phi_{\chi,k}^{i,n} = \theta_\chi^{i,n} - \phi_\chi^{i,n} - \varphi_{\chi,k}^{i,n}$, $L_k = L_{BS} L_{SU,\chi,k}$ is the overall path gain of the BS-STAR-RIS- U_k link, which can be expressed as

$$L_k = \frac{\rho_0^2}{d_{BS}^{\alpha_{BS}} d_{SU,\chi,k}^{\alpha_{SU}}}. \quad (7)$$

Here, d_{BS} is the distance between the BS and STAR-RIS and $d_{SU,\chi,k}$ is the distance between the STAR-RIS and the k th user in the transmission or reflection group. Additionally, ρ_0 , α_{BS} , and α_{SU} are the path gain at a reference distance of 1 meter, the path loss exponents associated with the BS-STAR-RIS and the STAR-RIS- U_k links, respectively.

By considering SIC, the SINR expression for user k , $k > 1$, after successfully detecting and subtracting the $k - 1$ users' signals before it, can be obtained as

$$\gamma_k = \frac{\rho \left| r_{\chi,k}^k \right|^2 a_k}{\rho \left| r_{\chi,k}^k \right|^2 \sum_{l=k+1}^K a_l + \rho \left| \sum_{\substack{i \in \mathbb{K}_\chi \\ i \neq k}} r_{\chi,k}^i \right|^2} + 1. \quad (8)$$

For the K th user, we have

$$\gamma_K = \frac{\rho \left| r_{\chi,K}^K \right|^2 a_K}{\rho \left| \sum_{\substack{i \in \mathbb{K}_\chi \\ i \neq K}} r_{\chi,K}^i \right|^2} + 1. \quad (9)$$

Considering the special case of $(K_t, K_r) = (1, 1)$, where one user is located in the transmission region and the other user is located in the reflection region, the SINR of the U_1 to detect its own signal is given by

$$\gamma_1 = \frac{\rho \left| r_{t,1}^1 \right|^2 a_1}{\rho \left| r_{t,1}^1 \right|^2 a_2 + 1}, \quad (10)$$

and the SINR of the U_2 to detect the U_1 's signal is given by

$$\gamma_2^1 = \frac{\rho \left| r_{r,2}^2 \right|^2 a_1}{\rho \left| r_{r,2}^2 \right|^2 a_2 + 1}, \quad (11)$$

finally, the SNR of the U_2 to detect its own signal is given by

$$\gamma_2 = \rho \left| r_{r,2}^2 \right|^2 a_2. \quad (12)$$

III. OUTAGE PROBABILITY ANALYSIS

In order to reveal its benefits, we examine the performance of the considered downlink STAR-RIS-assisted NOMA network analytically in terms of OP. In the following, we present the derivation of the exact and asymptotic expressions of the OP for the considered STAR-RIS aided NOMA network under different user deployments.

The OP of user k is the probability that the user cannot successfully detect and remove the signals of the $k - 1$ users before it and/or cannot detect its own signal. Let γ_{th}^j denote the SINR threshold for user k to detect user j 's signal, $1 \leq j \leq k$, thus, $E_{k \leftarrow j} = \left\{ \gamma_k^j < \gamma_{th}^j \right\}$ denotes the event that user k cannot detect user j 's signal. Thus, the OP for user k can be obtained as

$$OP_k = 1 - P_r(E_{k \leftarrow 1}^c \cap \dots \cap E_{k \leftarrow k}^c), \quad (13)$$

where $E_{k \leftarrow j}^c$ is the complement of the event $E_{k \leftarrow j}$.

Proposition 1. *The OP of the k th user is given by*

$$OP_k(\varrho_k^*) = 1 - Q_{\frac{1}{2}} \left(\frac{\mu_k}{\nu_k}, \frac{\sqrt{\varrho_k^*}}{\nu_k} \right) + \left(\frac{u_k^2}{\nu_k^2 + u_k^2} \right)^{\frac{1}{2}} e^{\frac{\varrho_k^*}{2u_k^2}} e^{-\frac{\mu_k^2}{2(\nu_k^2 + u_k^2)}} \times Q_{\frac{1}{2}} \left(\frac{\mu_k}{\nu_k} \sqrt{\frac{u_k^2}{\nu_k^2 + u_k^2}}, \sqrt{\frac{\varrho_k^* (\nu_k^2 + u_k^2)}{\nu_k^2 u_k^2}} \right), \quad (14)$$

where $\varrho_j^* = \max_{j=1, \dots, k} \{ \varrho_j \}$, $\varrho_j = \frac{\gamma_{th}^j}{\rho a_j - \rho \gamma_{th}^j \sum_j}$, $\mu_k = \frac{\pi}{4} \sqrt{L_k} N_\chi^k$, $\sum_j = \sum_{l=j+1}^K a_l$, $\nu_k = \sqrt{(1 - \frac{\pi^2}{16}) L_k N_\chi^k}$ and $u_k = \sqrt{0.5 \rho \varrho_k^* L_k (N_\chi - N_\chi^k)}$.

Proof. See Appendix A. ■

In order to gain further insights on the OP performance, we give the following Corollary.

Corollary 1. *Considering the asymptotic behavior of OP, for $\rho \rightarrow \infty$, i.e., $\varrho_k^* \rightarrow 0$, OP is given by*

$$OP_k^\infty = \left(\frac{\tilde{u}_k^2}{\nu_k^2 + \tilde{u}_k^2} \right)^{\frac{1}{2}} e^{-\frac{\mu_k^2}{2(\nu_k^2 + \tilde{u}_k^2)}}, \quad (15)$$

Proof. The proof follows directly from Proposition 1 by considering that $\varrho_k^* = 0$, then we have $Q_{\frac{1}{2}} \left(\frac{\mu_k}{\nu_k}, \frac{\sqrt{0}}{\nu_k} \right) = 1$, $\tilde{u}_k = \sqrt{0.5 \varrho_k^* L_k (N_\chi - N_\chi^k)}$ and $\varrho_k^* = \max_{j=1, \dots, k} \left\{ \frac{\gamma_{th}^j}{a_j - \gamma_{th}^j \sum_j} \right\}$. ■

From Corollary 1, it can be noticed that the OP reaches an error floor due to subsurface-interference when the transmit SNR increases.

Proposition 2. *In the case of a two-user STAR-RIS assisted NOMA network, $(K_t, K_r) = (1, 1)$, as shown in Fig. 2(a), the OP of the k th user can be expressed in closed-form as*

$$OP_k = 1 - Q_{\frac{1}{2}} \left(\frac{\mu_k}{\nu_k}, \frac{\sqrt{\varrho_k^*}}{\nu_k} \right). \quad (16)$$

Here, considering the asymptotic behavior, for $\rho \rightarrow \infty$, i.e., $\varrho_k^* \rightarrow 0$, we have $OP_k = 0$.

Proof. See Appendix B. ■

From Proposition 2, it can be noticed that in the case of a two-user STAR-RIS assisted NOMA network, since there is no subsurface-interference, the OP becomes zero in the high SNR region.

IV. PARTITIONING ALGORITHM

The objective of our partition algorithm is to find the proper number of transmitting/reflecting elements to be assigned to each user in order to maximize sum-rate and guarantee QoS requirements. In what follows, we present the partitioning algorithm considering different users' deployments.

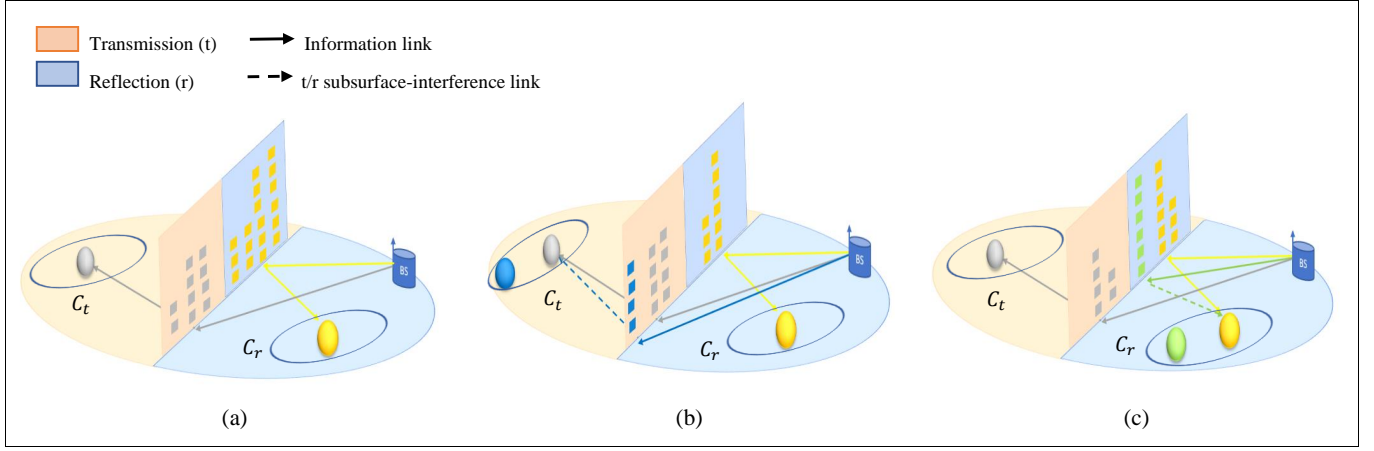


Fig. 2: STAR-RIS aided multi-user downlink communication systems (a) $(K_t, K_r) = (1, 1)$. (b) $(K_t, K_r) = (2, 1)$. (c) $(K_t, K_r) = (1, 2)$.

A. Multi-user STAR-RIS assisted NOMA system

In the case of a multi-user STAR-RIS assisted NOMA system, our partitioning algorithm is carried out in two stages. First, the STAR-RIS surface is partitioned into two parts, transmission and reflection parts, which contain all the elements that operate in transmission and reflection mode, respectively. Second, each STAR-RIS part is partitioned into subsurfaces, where each subsurface is allocated to serve a specific user located on the side of that part. In the following, both stages are explained in detail.

At the first stage, we assign temporary numbers of transmitting (\tilde{N}_t) and reflecting (\tilde{N}_r) STAR-RIS elements for the transmission and reflection STAR-RIS parts, respectively. Furthermore, the mode of the remaining STAR-RIS elements ($N - \tilde{N}_t - \tilde{N}_r$) will be selected further according to sum-rate and QoS requirements. \tilde{N}_t and \tilde{N}_r can be simply calculated, respectively as $\tilde{N}_t = K_t N_{thr}$ and $\tilde{N}_r = K_r N_{thr}$, where N_{thr} is the minimum number of STAR-RIS elements that needs to be allocated to each user in order to protect it from the subsurface-interference. We use Algorithm 1 to obtain the value of N_{thr} [19]. Particularly, Algorithm 1 utilizes a probabilistic approach, where (15) is used to obtain the probability that, for a given N_{thr} , the interference power is lower than the amplification power.

On the other hand, at the second stage, we aim to determine the proper number of transmitting/reflecting STAR-RIS elements that is required for each user to maximize the sum-rate and guarantee QoS for individual users. To achieve this goal, at first, Algorithm 2 is used to determine the number of STAR-RIS elements that need to be added to N_{thr} in order to fulfill the QoS requirement R_k^{min} for each user. According to (5), the cascaded channels' gains are proportionate with the number of transmitting or reflecting elements. Therefore, if the cascaded channels' gains are sorted as $|r_{\chi,1}^1|^2 \leq \dots \leq |r_{\chi,k}^k|^2 \leq \dots \leq |r_{\chi,K}^K|^2$, then the transmitting/reflecting STAR-RIS elements assigned for the users have to be also ordered as

Algorithm 1 Determination of minimum number of STAR-RIS elements that needs to be allocated to each user (N_{thr}).

Require: $L_{SU,\chi,k}$, K , N , ϵ .

1: Initialize $N_{thr} = 1$.

2: **repeat**

3: $\mu_k = \frac{\pi}{4} \sqrt{L_k N_{thr}}$, $\nu_k = \sqrt{(1 - \frac{\pi^2}{16}) L_k N_{thr}}$, $\tilde{u}_k = \sqrt{0.5 \rho_k^\dagger L_k (N - N_{thr})}$.

4: Obtain the asymptotic OP from (15):

$$OP_k^\infty = \left(\frac{\tilde{u}_k^2}{\nu_k^2 + \tilde{u}_k^2} \right)^{\frac{1}{2}} e^{-\frac{\mu_k^2}{2(\nu_k^2 + \tilde{u}_k^2)}}$$

5: $N_{thr} = N_{thr} + 1$.

6: **while** $OP_k^\infty \leq \epsilon$ and $KN_{thr} \leq N$.

7: **return** $N_{thr} = N_{thr} - 1$.

Algorithm 2 Determination of proper number of transmitting/reflecting STAR-RIS elements to be assigned to U_k (N_χ^k).

Require: N_{thr} , R_k^{min} .

1: Initialize $N_\chi^k = N_\chi^{k-1}$. If $k = 1$, then $N_\chi^1 = N_{thr}$.

2: **repeat**

3: Obtain the Ergodic rate in the high SNR values:

$R_k = E[\log_2(1 + \gamma_k^k)]$. Perform the expectation over 10^4 random channel realizations.

4: $N_\chi^k = N_\chi^k + 1$.

5: **while** $R_k < R_k^{min}$.

6: **return** $N_\chi^k = N_\chi^k - 1$.

$N_\chi^1 \leq \dots \leq N_\chi^k \leq \dots \leq N_\chi^K$, which is ensured by Algorithm 2. Next, in order to maximize the sum-rate, the remaining STAR-RIS elements are added to the closest user to the BS, U_K , which can eliminate the interference of all other users. At the end, the proper values of N_t and N_r are updated, respectively as $N_t = \sum_{k=1}^{K_t} N_t^k$ and $N_r = \sum_{k=K_t+1}^K N_r^k$.

TABLE I: Parameters used in simulations for the three cases.

User locations	Case 1: U_1 is located in C_t and U_2 is located in C_r . Case 2: U_1 and U_2 are located in C_t , and U_3 is located in C_r . Case 3: U_1 is located in C_t , and U_2 and U_3 are located in C_r .
Power allocation coefficients	Case 1: $(a_1, a_2) = (0.6, 0.4)$ Case 2: $(a_1, a_2, a_3) = (0.6, 0.3, 0.1)$ Case 3: $(a_1, a_2, a_3) = (0.6, 0.3, 0.1)$
Target threshold SINR values	Case 1: $(\gamma_{th}^1, \gamma_{th}^2) = (1, 1)$ Case 2: $(\gamma_{th}^1, \gamma_{th}^2, \gamma_{th}^3) = (0.7, 0.7, 0.7)$ Case 3: $(\gamma_{th}^1, \gamma_{th}^2, \gamma_{th}^3) = (0.5, 0.5, 0.3)$
Distances (in meters)	Case 1: $(d_{BS}, d_{SU,t,1}, d_{SU,r,2}) = (50, 50, 40)$ Case 2: $(d_{BS}, d_{SU,t,1}, d_{SU,t,2}, d_{SU,r,3}) = (20, 50, 40, 30)$ Case 3: $(d_{BS}, d_{SU,t,1}, d_{SU,r,2}, d_{SU,r,3}) = (20, 50, 40, 30)$

B. Two-user STAR-RIS assisted NOMA system

As shown in Fig. 2(a), for the case of a two-user STAR-RIS assisted NOMA system, one user is located in C_t and the other user is located in C_r . Since, in this case, there is no subsurface interference, we skip the first stage of the partitioning process and start directly from the second one. That is, Algorithm 2 is directly applied to fulfill the QoS requirement for U_1 , with $N_{thr} = 1$ and (10) is used to obtain γ_k^k . Next, the remaining elements need to be allocated to U_2 , assuming N is large enough to fulfill both users' QoS requirements.

V. NUMERICAL RESULTS

In this section, the performance of the considered downlink STAR-RIS-assisted multi-user wireless networks is presented via computer simulations in order to validate our theoretical analysis. We consider three cases, $(K_t, K_r) = (1, 1)$, $(K_t, K_r) = (2, 1)$ and $(K_t, K_r) = (1, 2)$, which shown in Figs. 2(a)-(c), respectively. For each case, user locations, power allocation coefficients, corresponding target threshold SINR values, distances between the BS and STAR-RIS, and STAR-RIS and users are given in Table I. For all cases, the path gain at a reference distance of 1 meter is assumed as $\rho_0 = -30$ dB and the path loss exponents associated with the BS-STAR-RIS and the STAR-RIS-User links are given as $(\alpha_{BS}, \alpha_{SU}) = (2, 2)$ unless otherwise stated. Furthermore, we compare the proposed system with two benchmark systems, namely the classical OMA and PD-NOMA systems by considering the same simulation parameters. Particularly, for the classical PD-NOMA system, we use the same power allocation that we use in the proposed system. On the other side, for the classical OMA system, we use the time division multiple access (TDMA) scheme, where the time slot allocation equals the power allocation in NOMA case; therefore, we always have the time slots $t_1 = a_1$, $t_2 = a_2$, and $t_3 = a_3$. For the benchmark systems, the BS- U_k path gain is obtained as $L_k = \frac{\rho_0}{d_k^\alpha}$, where d_k is the BS- U_k distance and $\alpha = 3.5$ [21].

A. Case 1: $(K_t, K_r) = (1, 1)$

Figs. 3 and 4 show the OP and sum-rate performance of the STAR-RIS assisted NOMA network for different number of STAR-RIS elements $N \in \{64, 128, 256\}$, respectively. According to Algorithm 2, the number of the transmitting STAR-RIS elements for U_1 and the number of the reflecting STAR-RIS elements for U_2 are determined, respectively as

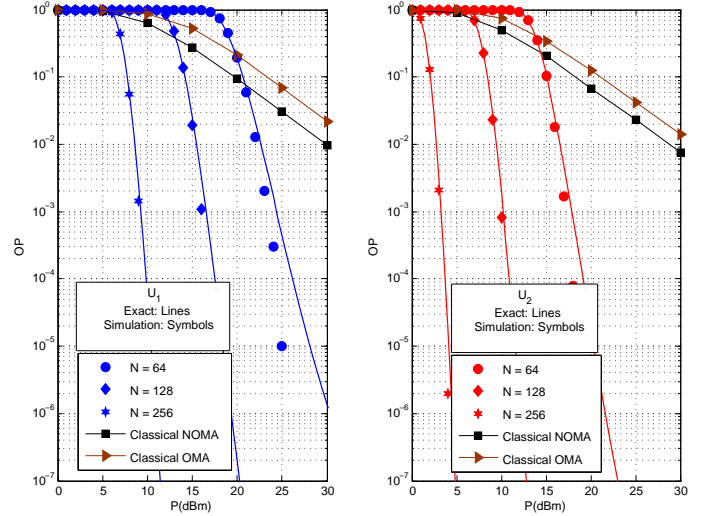


Fig. 3: The outage probability versus P for different N in the case of $(K_t, K_r) = (1, 1)$.

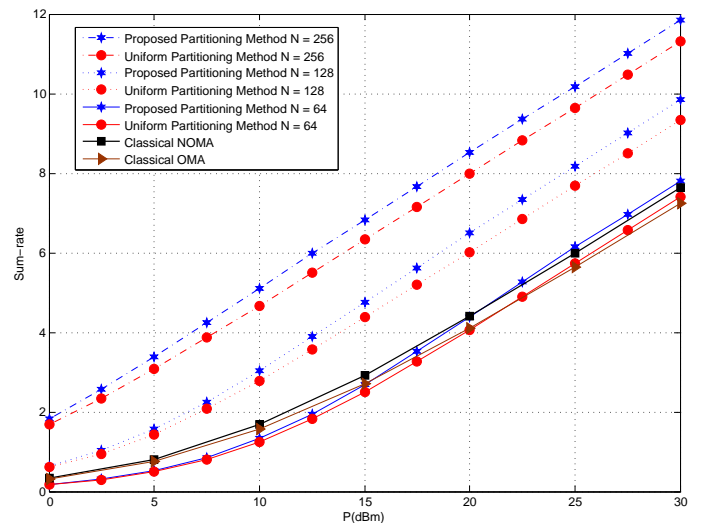


Fig. 4: The sum-rate versus P for different N in the case of $(K_t, K_r) = (1, 1)$.

$N_t^1 = \{26, 51, 102\}$ and $N_r^2 = \{38, 77, 154\}$. As seen from Fig. 3, our theoretical result in (16) using the CLT is considerably accurate for increasing N values. In addition, the OP performance enhances as number of STAR-RIS elements

increases. For instance, to achieve $OP_1 = 10^{-3}$, 10 dBm and 5 dBm gain advantages are obtained in P for $N = 128$ over $N = 64$ and $N = 256$ over 128, respectively. On the other hand, to achieve $OP_2 = 10^{-3}$, about 7.5 dBm and 7 dBm gain advantages are observed in P for $N = 128$ over $N = 64$ and $N = 256$ over 128, respectively. We can clearly notice from Fig. 4 that the sum-rate proportionally increases as P increases. This is because the sum-rate depends remarkably on the strongest user (U_2) and in this case, U_2 does not suffer from any subsurface-interference. In addition, the proposed partitioning method outperforms the uniform partitioning method. Also, from both figures, we can see the superiority of our proposed system over the classical NOMA and OMA particularly by increasing the total number of the elements of STAR-RIS.

B. Case 2: $(K_t, K_r) = (2, 1)$

Figs. 5 and 6 demonstrate the performance of the STAR-RIS assisted NOMA network in terms of OP and sum-rate, respectively for different number of STAR-RIS elements. The number of transmitting/reflecting STAR-RIS elements assigned for each user is provided in Table II. It can be seen from Fig. 5 that when P increases, the OP_1 and OP_2 reach an error floor due to subsurface-interference. On the other hand, OP_3 does not reach error floor since U_3 does not suffer from any subsurface-interference. Compared to the classical NOMA and OMA, the proposed system is always better for U_3 in the whole P range as well as U_1 and U_2 except in the high P regime. As shown in Fig. 6, the sum-rate still proportionally increases as P increases since the strongest user (U_3) does not suffer from the subsurface-interference. Furthermore, the STAR-RIS requires about $N = 90$ and $N = 150$ elements to outperform classical OMA and classical NOMA, respectively.

C. Case 3: $(K_t, K_r) = (1, 2)$

Figs. 7 and 8 present the OP and sum-rate performance of the STAR-RIS assisted NOMA network for different number of STAR-RIS elements. The number of transmitting/reflecting STAR-RIS elements assigned for each user is provided in Table III. From Fig. 7, it is clearly observed that the OP_2 and OP_3 reach an error floor due to subsurface-interference. On the other hand, the OP_1 does not reach error floor since U_1 does not suffer from any subsurface-interference. As seen from Fig. 8, the sum-rate saturates in the high P region. This is because the strongest user (U_3) suffers from subsurface-interference, which significantly affect the sum-rate performance. The proposed partitioning approach is also superior to the uniform partitioning approach. Although classical NOMA and OMA outperform the proposed system in the high SNR region, with a large number of STAR-RIS elements, the proposed system can outperform both classical systems. For instance, the proposed system requires more than $N = 390$ elements to outperform both classical systems.

VI. CONCLUSION

In this work, we have proposed a STAR-RIS-assisted NOMA network where the MS operating protocol is utilized

TABLE II: Number of STAR-RIS elements assigned for each user in Case 2 when $N \in \{60, 90, 120, 150\}$.

N	N_t^1	N_r^2	N_r^3	N_t	N_r
60	16	20	24	36	24
90	24	30	36	54	36
120	32	40	48	72	48
150	36	50	64	86	64

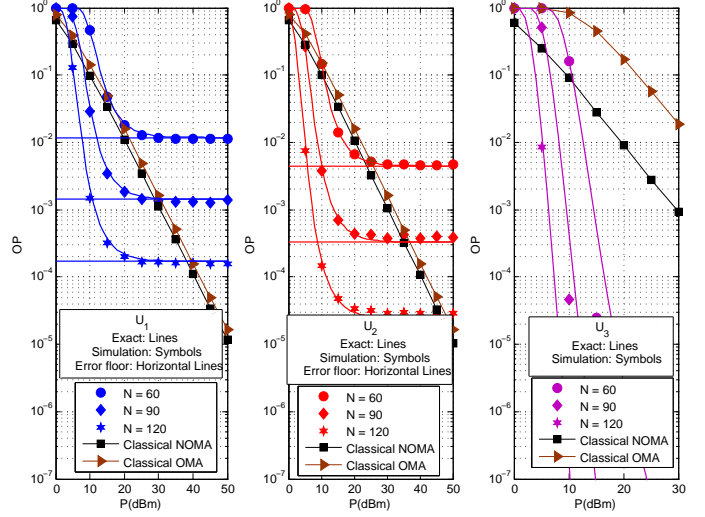


Fig. 5: The outage probability versus P for different N in the case of $(K_t, K_r) = (2, 1)$.

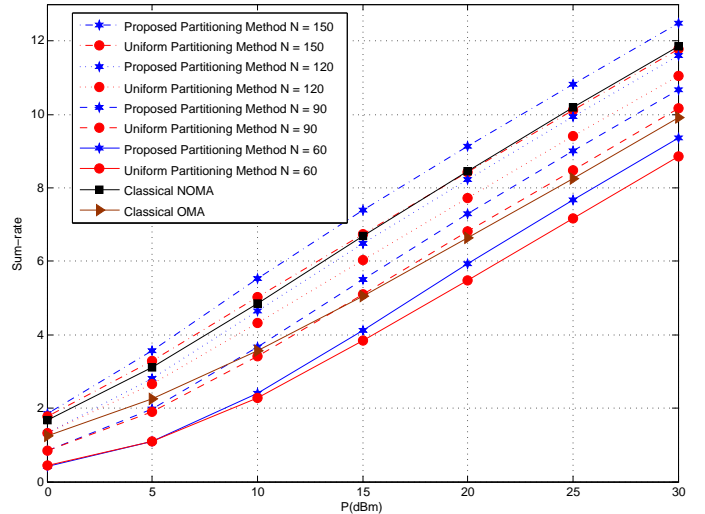


Fig. 6: The sum-rate versus P for different N in the case of $(K_t, K_r) = (2, 1)$.

to extend the coverage area of classical RIS. Next, we have designed a novel STAR-RIS partitioning algorithm to serve NOMA users on both sides of the STAR-RIS. The proposed algorithm aims to determine the proper number of transmitting/reflecting STAR-RIS elements that requires to be allocated to each user to maximize the sum-rate while fulfilling the QoS requirement. For different NOMA user deployments, we have provided a closed-form expression of the exact OP. Then, an asymptotic analysis has been conducted in order to study the system performance at the high SNR. We note that the OP

TABLE III: Number of STAR-RIS elements assigned for each user in Case 3 when $N \in \{60, 90, 120, 180\}$.

N	N_k^1	N_r^2	N_r^3	N_t	N_r
60	16	20	24	16	44
90	19	30	41	19	71
120	22	40	58	22	98
180	35	60	85	35	145
390	52	130	208	52	338

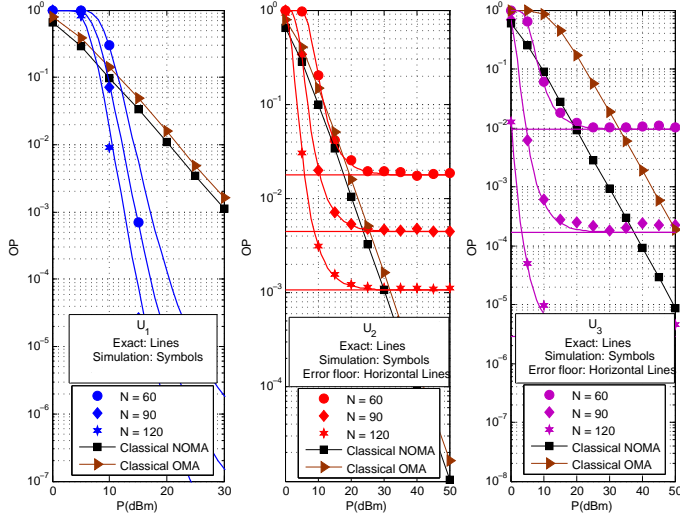


Fig. 7: The outage probability versus P for different N in the case of $(K_t, K_r) = (1, 2)$.

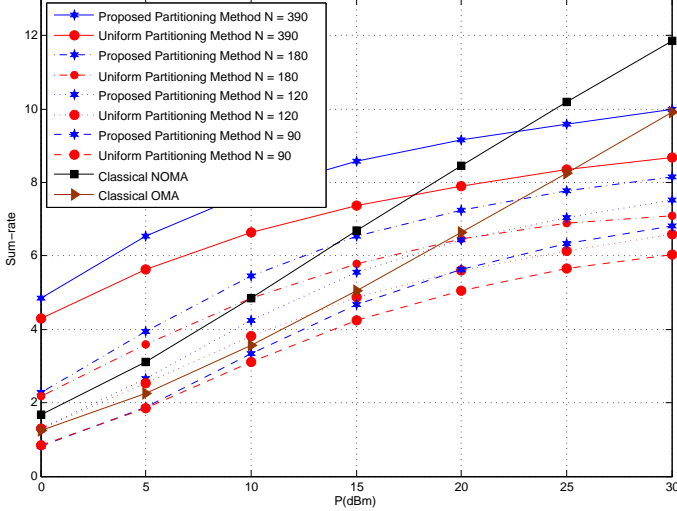


Fig. 8: The sum-rate versus P for different N in the case of $(K_t, K_r) = (1, 2)$.

reaches an error floor in the high SNR region due to the impact of the STAR-RIS's subsurface-interference and it can be reduced by increasing the number of STAR-RIS elements. Finally, simulation results have validated that the proposed partitioning algorithm outperforms the uniform partitioning algorithm. Moreover, the proposed system can achieve better performance in terms of OP and sum-rate than the classical NOMA and OMA. We conclude that the use of STAR-RIS NOMA has the potential to provide an enhanced version of

classical NOMA systems, where unlike the classical RIS, the STAR-RIS doubled the coverage area. Furthermore, in addition to the STAR-RIS MS mode, our proposed partitioning scheme has added more degrees of freedom to the system design, compared to the classical PD-NOMA protocol, by flexibly and dynamically allocating the physical resources (STAR-RIS elements) among users. In the future, we extend the proposed system to STAR-RIS aided NOMA networks with multiple antennas.

APPENDIX A PROOF OF PROPOSITION 1

By considering (3), $E_{k \leftarrow j}^c$ can be expressed as

$$E_{k \leftarrow j}^c = \left\{ \frac{\rho |r_{\chi,k}^k|^2 a_j}{\rho |r_{\chi,k}^k|^2 \sum_j + \rho \left| \sum_{i \in \mathbb{K}_\chi, i \neq k} r_{\chi,k}^i \right|^2 + 1} > \gamma_{th}^j \right\} \stackrel{(c)}{=} \left\{ |r_{\chi,k}^k|^2 > \rho \varrho_j \left| \sum_{i \in \mathbb{K}_\chi, i \neq k} r_{\chi,k}^i \right|^2 + \varrho_j \right\}, \quad (17)$$

where $\sum_j = \sum_{l=j+1}^K a_l$, $\varrho_j = \frac{\gamma_{th}^j}{\rho a_j - \rho \gamma_{th}^j \sum_j}$ and the step (c) is obtained under the condition of $a_j > \gamma_{th}^j \sum_{l=j+1}^K a_l$. Now, substituting (17) into (13) and defining $\varrho_j^* = \max_{j=1, \dots, k} \{\varrho_j\}$, then the OP of the k th user can be stated as

$$\begin{aligned} OP_k &= 1 - P_r \left(|r_{\chi,k}^k|^2 > \rho \varrho_k^* \left| \sum_{i \in \mathbb{K}_\chi, i \neq k} r_{\chi,k}^i \right|^2 + \varrho_k^* \right) \\ &= P_r \left(|r_{\chi,k}^k|^2 < \rho \varrho_k^* \left| \sum_{i \in \mathbb{K}_\chi, i \neq k} r_{\chi,k}^i \right|^2 + \varrho_k^* \right) \\ &= F_{R_k}(\varrho_k^*). \end{aligned} \quad (18)$$

Here, $R_k = |r_{\chi,k}^k|^2 - \rho \varrho_k^* \left| \sum_{i \in \mathbb{K}_\chi, i \neq k} r_{\chi,k}^i \right|^2 = |r_{\chi,k}^k|^2 - \left| \sqrt{\rho \varrho_k^*} \sum_{i \in \mathbb{K}_\chi, i \neq k} r_{\chi,k}^i \right|^2$. It is worth noting that the BS-STAR-RIS- U_k cascaded channel gains are sorted as $|r_{\chi,1}^1|^2 \leq \dots \leq |r_{\chi,k}^k|^2 \leq \dots \leq |r_{\chi,K}^K|^2$, where this users' order can be always guaranteed by allocating the proper STAR-RIS elements for each user.

Noting $\zeta_{\chi}^{i,n}$ and $\eta_{\chi,k}^{i,n}$ are independently Rayleigh distributed random variables (RVs) with a mean $E[\zeta_{\chi}^{i,n}] = E[\eta_{\chi,k}^{i,n}] = \frac{\sqrt{\pi}}{2}$ and a variance $\text{VAR}[\zeta_{\chi}^{i,n}] = \text{VAR}[\eta_{\chi,k}^{i,n}] = 1 - \frac{\pi}{4}$. Then, $E[\zeta_{\chi}^{i,n} \eta_{\chi,k}^{i,n}] = \frac{\pi}{4}$ and $\text{VAR}[\zeta_{\chi}^{i,n} \eta_{\chi,k}^{i,n}] = 1 - \frac{\pi^2}{16}$. According to the CLT, for $N_{\chi}^k \gg 1$, the cascaded channel $r_{\chi,k}^k$ converges to Gaussian RV. Thus,

$$r_{\chi,k}^k \sim \mathcal{N} \left(\frac{\pi}{4} \sqrt{L_k} N_{\chi}^k, \left(1 - \frac{\pi^2}{16} \right) L_k N_{\chi}^k \right). \quad (19)$$

In addition, for $N_\chi - N_\chi^k \gg 1$, $\sum_{i \neq k}^{K_\chi} r_{\chi,k}^i$ converges to Gaussian RV. So,

$$\sum_{\substack{i \in \mathbb{K}_\chi \\ i \neq k}} r_{\chi,k}^i \sim \mathcal{CN}(0, L_k(N_\chi - N_\chi^k)). \quad (20)$$

It is noticed that $|r_{\chi,k}^k|^2$ is a non-central chi-square RV with one degree of freedom and $|\sum_{i \in \mathbb{K}_\chi, i \neq k} r_{\chi,k}^i|^2$ is a central chi-square RV with two degrees of freedom. Hence, R_k is the difference of a non-central and central independent chi-square RVs and by using its corresponding CDF $F_{R_k}(x)$ [20], the OP of the k th user can be expressed in closed-form as in (14).

APPENDIX B PROOF OF PROPOSITION 2

By using (11), the OP of the k th user can be stated as

$$\begin{aligned} OP_k &= P_r \left(\frac{\rho |r_{\chi,k}^k|^2 a_j}{\rho |r_{\chi,k}^k|^2 \sum_j + 1} < \gamma_{th}^j \right) \\ &= P_r \left(|r_{\chi,k}^k|^2 \left(\rho a_j - \rho \gamma_{th}^j \sum_j \right) < \gamma_{th}^j \right) \\ &= P_r \left(|r_{\chi,k}^k|^2 < \varrho_k^* \right) \\ &= F_{|r_{\chi,k}^k|^2}(\varrho_k^*). \end{aligned} \quad (21)$$

Recall, $|r_{\chi,k}^k|^2$ is a non-central chi-square RV with one degree of freedom and its corresponding CDF can be written as

$$F_{|r_{\chi,k}^k|^2}(x) = 1 - Q_{\frac{1}{2}} \left(\frac{\mu_k}{\nu_k}, \frac{\sqrt{x}}{\nu_k} \right). \quad (22)$$

Then, by using (22), the OP of the k th user can be stated as in (16).

REFERENCES

- [1] Y. Liu *et al.*, "Reconfigurable intelligent surfaces: principles and opportunities," *IEEE Commun. Surveys & Tuts.*, vol. 23, no. 3, pp. 1546-1577, 3rd quarter 2021.
- [2] S. Basharat *et al.*, "Reconfigurable intelligent surfaces: potentials, applications, and challenges for 6G wireless networks," July 2021. [Online]. Available: <https://arxiv.org/abs/2107.05460v1>.
- [3] Q. Wu and R. Zhang, "Towards smart and reconfigurable environment: intelligent reflecting surface aided wireless network," *IEEE Commun. Mag.*, vol. 58, no. 1, pp. 106-112, Jan. 2020.
- [4] E. Basar and H. V. Poor, "Present and future of reconfigurable intelligent surface-empowered communications", *accepted to IEEE Signal Process. Mag.*, Aug. 2021.
- [5] Y. Liu *et al.*, "STAR: Simultaneous transmission and reflection for 360 coverage by intelligent surfaces," Mar. 2021. [Online]. Available: <https://arxiv.org/abs/2103.09104v2>.
- [6] Y. Liu *et al.*, "Application of NOMA in 6G networks: future vision and research opportunities for next generation multiple access," Mar. 2021. [Online]. Available: <https://arxiv.org/abs/2103.02334v1>.
- [7] M. Aldababsa *et al.*, "A tutorial on non-orthogonal multiple access (NOMA) for 5G and beyond", *J. Wireless Commun. Mobile Computing*, June 2018.
- [8] S. Islam *et al.*, "Power-domain non-orthogonal multiple access (NOMA) in 5G systems: potentials and challenges," *IEEE Commun. Surveys & Tuts.*, vol. 19, no. 2, pp. 721-742, 2nd quarter 2017.

- [9] J. Xu *et al.*, "STAR-RISs: simultaneous transmitting and reflecting reconfigurable intelligent surfaces," Mar. 2021. [Online]. Available: <https://arxiv.org/abs/2101.09663v2>.
- [10] X. Mu *et al.*, "Simultaneously transmitting and reflecting (STAR) RIS aided wireless communications," Apr. 2021. [Online]. Available: <https://arxiv.org/abs/2104.01421v1>.
- [11] H. Niu *et al.*, "Simultaneous transmission and reflection reconfigurable intelligent surface assisted MIMO systems," June 2021. [Online]. Available: <https://arxiv.org/abs/2106.09450v1>.
- [12] J. Xu *et al.*, "Simultaneously transmitting and reflecting (STAR) intelligent omni-surfaces, their modeling and implementation," Sept. 2021. [Online]. Available: <https://arxiv.org/abs/2108.06233v2>.
- [13] C. Wu *et al.*, "Coverage characterization of STAR-RIS networks: NOMA and OMA," *IEEE Commun. Lett.*, June 2021.
- [14] T. Hou *et al.*, "A jointly design for STAR-RIS enhanced NOMA-CoMP networks: a simultaneously-signal-enhancement-and-cancellation-based (SSECB) design," May 2021. [Online]. Available: <https://arxiv.org/abs/2105.00404v2>.
- [15] J. Zuo *et al.*, "Joint design for simultaneously transmitting and reflecting (STAR) RIS assisted NOMA systems," June 2021. [Online]. Available: <https://arxiv.org/abs/2106.03001v1>.
- [16] W. Ni *et al.*, "STAR-RIS enabled heterogeneous networks: ubiquitous NOMA communication and pervasive federated learning," June 2021. [Online]. Available: <https://arxiv.org/abs/2106.08592v2>.
- [17] C. Zhang *et al.*, "STAR-IOS aided NOMA networks: channel model approximation and performance analysis," July 2021. [Online]. Available: <https://arxiv.org/abs/2107.01543v1>.
- [18] Z. Xie *et al.*, "STAR-RIS aided NOMA in multi-cell networks: a general analytical framework with Gamma distributed channel modeling," Aug. 2021. [Online]. Available: <https://arxiv.org/abs/2108.06704v1>.
- [19] A. Khaleel and E. Basar, "A novel NOMA solution with RIS partitioning," June 2021. [Online]. Available: <https://arxiv.org/abs/2011.10977v2>.
- [20] M. Simon, *Probability Distributions Involving Gaussian Random Variables*, New York, NY, USA: Springer, 2002.
- [21] Q. Wu and R. Zhang, "Intelligent reflecting surface enhanced wireless network via joint active and passive beamforming," *IEEE Trans. Wireless Commun.*, vol. 18, no. 11, pp. 5394-5409, Nov. 2019.